

Incoherent π^0 photoproduction from complex nucleiT. E. Rodrigues,¹ J. D. T. Arruda-Neto,^{1,2} J. Mesa,¹ C. Garcia,¹ K. Shtejer,^{1,3} D. Dale,⁴ and I. Nakagawa⁴¹*Instituto de Física da Universidade de São Paulo, P.O. Box 66318, CEP 05315-970, São Paulo, Brazil*²*Universidade de Santo Amaro/UNISA, São Paulo, Brazil*³*Center of Applied Studies for Nuclear Developments (CEADEN), Havana, Cuba*⁴*Department of Physics and Astronomy, University of Kentucky, Lexington, Kentucky, 40506*

(Received 5 November 2004; published 19 May 2005)

Incoherent π^0 photoproduction from nuclei is evaluated via a multicolisional intranuclear cascade framework. In-medium modifications are taken into account, including a realistic dynamical treatment of multiple πN and ΔN scattering processes throughout the cascade. This time-dependent analysis yields structures in the ^{12}C π^0 differential cross section both in the Δ region and in the photon energy range from 5 to 6 GeV, with the former in very nice agreement with recent results from Mainz Microtron. For heavy nuclei, however, such structures disappear because of a more effective Fermi motion and a relatively higher final state interaction of the produced pions as they exit the nucleus. The calculation of the incoherent part of the total π^0 photoproduction propitiates a clean and powerful kinematical separation from competitive (electromagnetic/nuclear) production processes, which currently is a theoretical challenge for the PrimEx experiment at the Jefferson Lab.

DOI: 10.1103/PhysRevC.71.051603

PACS number(s): 25.20.Lj, 21.65.+f, 24.10.-i, 25.80.Ls

Various experiments have been recently proposed in an effort to investigate in-medium modifications in meson photoproduction from complex nuclei. Single π^0 , double π^0 , and $\pi^0\pi^{+-}$ photoproduction channels from 200 to 800 MeV in nuclei were explored by the Mainz Microtron (MAMI) collaboration [1]. In these experiments, they were able to separate the incoherent and coherent parts of the single π^0 differential cross section near the Δ (1232), where the incoherent contribution exhibited remarkable structures for the ^{12}C . Such an intriguing result propitiates an accurate verification of the available models in describing nuclear matter effects. Another interesting result showed up in the total photoabsorption cross section, where the peak of the second resonance, the so-called $N(1520)$, is highly suppressed for both light and heavy nuclei.

Another example of the in-medium influence in the higher photon energy regime, is the incoherent π^0 photoproduction background at forward polar angles when extracting the π^0 lifetime via the Primakoff effect [2,3], as proposed by the PrimEx collaboration at the Jefferson Lab [4]. In fact, one of the major theoretical challenges in this experiment is the kinematical separation of the electromagnetic production, which comes from the coupling of the incident photon with the Coulomb field of the nucleus, from competitive (coherent and incoherent) nuclear mechanisms. For more details see Ref. [5] and references therein.

In this Rapid Communication we report for the first time a full dynamical model, based on a time-dependent multicolisional intranuclear cascade framework, to calculate the incoherent π^0 photoproduction from the pion threshold up to 6 GeV incident photon energies. The model is an extension of the original MCMC (Monte Carlo Multi-Collisional) model [6–9] with a novel approach focused on the quasideuteron energy region [10]. This newest version has incorporated substantial theoretical improvements with respect to similar cascade calculations [11] and has completely eliminated the

long-standing spurious depletion of the Fermi-sphere by introducing a nonstochastic treatment of the Pauli-blocking mechanism. This method effectively updates the nuclear matter density fluctuations in time, representing thus an advantage in comparison with other existing transport calculations, such as the sophisticated BUU (Boltzmann-Uehling-Uhlenbeck) model [12,13]. For details see Ref. [10] and references therein. Some special features used in the present Monte Carlo calculation are as follows: (i) two possible nuclear ground state configurations (i.e., the Fermi gas configuration for heavy nuclei and the shell model for light nuclei); (ii) in-medium quantum effects, such as a realistic Pauli-blocking mechanism which takes into account the dynamical evolution of p-h excitations during the cascade stage, and energy and momentum conservation during the emission of particles; (iii) all the dynamical information from the meson production vertex in the first interaction mechanism; (iv) a consistent calculation of the π -nucleus and Δ -nucleus final state interactions (FSI) via a state-of-the-art analysis of multiple πN and ΔN scatterings throughout the cascade, and (v) multiple neutral and charged pion production final state processes in the cascade dynamics.

The scope of the present work is to explore the in-medium effects in neutral pion photoproduction from nuclei in a broad energy range. In this regard, we have chosen two particular incoherent mechanisms: (i) inclusive π^0 photoproduction near the Δ resonance ($E_\gamma \approx 0.3$ GeV) and covering the full angular distribution range and (ii) single π^0 photoproduction at higher energies ($4.0 \leq E_\gamma \leq 6.0$ GeV) and low scattering angles. Such particular choice is quite convenient since the elementary mechanisms, which work as inputs to our cascade calculation, are well understood and constrained by the available experimental data. It is worth noticing, however, that the method described in this article is completely insensitive to this arbitrary kinematical choice, even though the final results are tightly connected with the input parametrization.

For incident photon energies near the Δ region ($E_\gamma \approx 0.3$ GeV) we have considered only the $P_{33}(1232)$ contribution to π^0 photoproduction, because the Born term can be safely neglected, as indicated by the unitary isobar model predictions [14]. The pion pole and Kroll-Rudermann contributions are relevant only for charged pion production and have been neglected in our approach. An additional contribution to neutral pions may also appear because of charge exchange mechanisms following a charged pion production. However, as shown, such a process is much less likely to occur than a Δ reexcitation, which makes neglecting it a quite good approximation.

The differential cross section for the elementary π^0 photoproduction near the Δ resonance can be parameterized in the following form:

$$\frac{d\sigma_N}{d\Omega} = \frac{q}{k} \sum_{n=0}^4 a_n \cos(\theta^*)^n, \quad (1)$$

where q and k are the meson and photon momenta in the center-of-mass of the s -channel and θ^* is the pion polar angle in this reference system, with the parameters a_n representing the best fit values for the available data [15–20]. The result for this parametrization and the corresponding data are shown in Fig. 1, where the solid histogram represents the Monte Carlo generated input.

The produced $\Delta^{0,+}$ resonance state interacts within the nuclear field via an n -body ΔN scattering scenario until it decays. The Δ decay is sampled accordingly with Eq. (1), and the final states $\pi^0 n$, $\pi^- p$, $\pi^+ n$, and $\pi^0 p$ are affected by nuclear medium if the decay occurs inside the nucleus.

The incoherent π^0 photoproduction at forward angles and higher energies ($E_\gamma \gtrsim 4.0$ GeV), which is the main subject of this article, has completely different kinematics from multiple

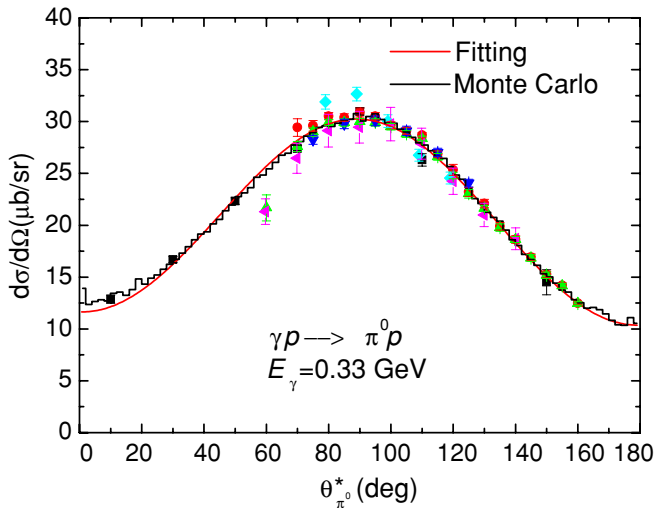


FIG. 1. (Color online) The elementary $\gamma p \rightarrow \pi^0 p$ differential cross section for $E_\gamma = 0.33$ GeV in the center-of-mass of the s -channel. Data points are as follows: squares [15], circles [16], up-triangles [17], down-triangles [18], diamonds [19], and left-triangles [20]. The red line is the fitting of Eq. (1) and the black histogram is the Monte Carlo input.

meson production channels and is much more sensitive to the single π^0 photoproduction from the proton.

The differential cross section for meson photoproduction from the nucleon at small angles in the center-of-mass of the s -channel can be written as [21] follows¹:

$$\frac{d\sigma_N}{d\Omega} \approx |f_1 - f_2|^2 + \frac{\theta^{*2}}{2} [|f_3 + f_4|^2 + 2 \operatorname{Re}(f_1^* f_2 + f_1^* f_4 + f_2^* f_3)], \quad (2)$$

where the f_i 's are the Pauli-type amplitudes [22]. These amplitudes are functions of the invariant amplitudes $A_i = A_i(s, t)$, with $s = (k + p_1)^2$ and $t = (k - p_2)^2$ representing the Mandelstam variables, and p_1 and p_2 are the initial and final four-momentum of the nucleon. The relationship between the Pauli-type amplitudes f_i 's and the analytical amplitudes A_i 's is given by Refs. [21,22], where we have assumed that the initial and final nucleon energies are the same ($t \ll 1$).

By decomposing the invariant amplitudes A_i in terms of regularized and parity-conserving t -channel helicity amplitudes F_i , we obtain² the following [23,24]:

$$A_1 = -\frac{t F_1 + 2m_N F_3}{t - 4m_N^2} \quad (3)$$

$$A_2 = \frac{F_1}{t - 4m_N^2} + \frac{1}{t} \left[F_2 + \frac{2m_N F_3}{t - 4m_N^2} \right] \quad (4)$$

$$A_3 = -F_4 \quad (5)$$

$$A_4 = -\frac{2m_N F_1 + F_3}{t - 4m_N^2}, \quad (6)$$

where m_N is the nucleon mass.

The amplitudes F_2 (unnatural parity exchange) and F_3 (natural parity exchange) receive contributions from different trajectories, whereas the amplitudes A_i are known to be free of kinematical singularities [21]. Because Eq. (4) has a pole at $t = 0$, one is forced to postulate the so-called “conspiracy relation” at zero momentum transfer³:

$$F_3(s, t = 0) = 2m_N F_2(s, t = 0). \quad (7)$$

Using Eqs. (3)–(7) and writing Eq. (2) in terms of the F_i 's, we have the following [23]:

$$\frac{d\sigma_N}{dt} \approx \frac{\pi}{k^2} \frac{d\sigma_N}{d\Omega} = \frac{1}{32\pi} \left\{ \frac{F_3^2}{2m_N^2} - \left[t + \left(\frac{m_\pi^2}{2k} \right)^2 \right] \times \left[F_4^2 + \frac{F_1^2}{4m_N^2} + \frac{F_3^2}{16m_N^4} + \frac{F_1 F_3}{2m_N k \sqrt{s}} \right] \right\}, \quad (8)$$

where m_π is the meson mass.

¹To obtain Eq. (2) one has to expand Eq. (9.6) from Ref. [21] for $\theta \ll 1$ and make $q \approx k$.

²The pion pole could contribute for neutral pions in the event of a charge-exchange process. However, for high-incident energies, such process is completely negligible (see Fig. 3).

³This relation is similar to the one obtained by Ball *et al.* [24]. The difference comes from the pion exchange contribution.

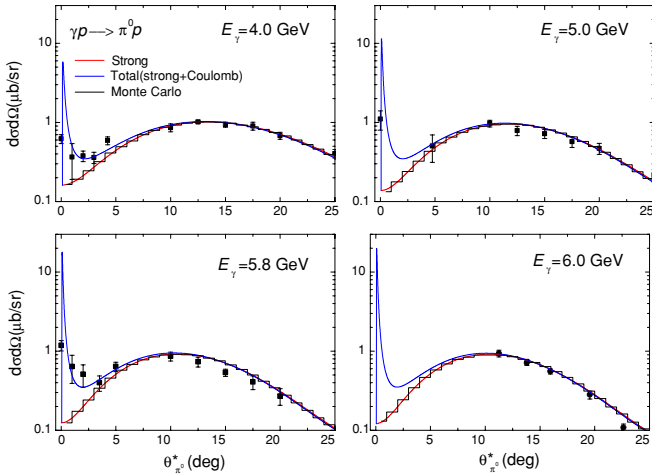


FIG. 2. (Color online) The elementary $\gamma p \rightarrow \pi^0 p$ differential cross section in the energy range $4.0 \leq E_\gamma \leq 6.0$ GeV in the center-of-mass of the s -channel. The strong contribution is shown by the red line, whereas the total (strong + Coulomb) is shown by the blue line. The data were taken from squares [25] and circles [26]. The black histogram is the Monte Carlo input.

The helicity amplitudes F_i are then calculated using the standard Regge-pole model, including ω - and ρ -meson trajectories and taking into account the reggeon cuts [25]. Within this approach, the amplitudes F_i 's lose the property of definite parity and also become finite at zero momentum transfer. The photon exchange amplitude F^C , which is the elementary Primakoff effect, plays an essential role at low momentum transfer and has to be subtracted from the total π^0 elementary photoproduction, because only the strong part should be included in the cascade input.

So, neglecting B-exchange ($F_4 = 0$) and adding constructively the cuts and Coulomb contributions, we have the

following [23,25]:

$$F_1 \rightarrow F_1 + F_1^{\text{cut}} + F_1^C, F_3 \rightarrow F_3^{\text{cut}}, \quad (9)$$

where

$$F_1(s, t) = \frac{\sqrt{2}}{m_N} \gamma_1 \frac{1 - e^{-i\pi\alpha(t)}}{\sin[\pi\alpha(t)]} \alpha(t)[1 + \alpha(t)] \times [2 + \alpha(t)] \left(\frac{s}{s_0}\right)^{\alpha(t)-1}, \quad (10)$$

$$F_1^{\text{cut}}(s, t) = \frac{\sqrt{2}}{m_N} \gamma_1^{\text{cut}} \frac{1 - e^{-i\pi\alpha(0)}}{\sin[\pi\alpha(0)]} \left(\frac{s}{s_0}\right)^{\alpha(0)-1} \frac{e^{at}}{\ln\left(\frac{s}{s_0}\right)}, \quad (11)$$

$$F_1^C(s, t) = -\frac{2m_N}{t} 0.0543 \sqrt{\Gamma_{\gamma\gamma}} G_E(t),$$

and

$$F_3^{\text{cut}}(s, t) = 2\sqrt{2}\gamma_3^{\text{cut}} \frac{1 - e^{-i\pi\alpha(0)}}{\sin[\pi\alpha(0)]} \left(\frac{s}{s_0}\right)^{\alpha(0)-1} \frac{e^{at}}{\ln\left(\frac{s}{s_0}\right)}. \quad (12)$$

The Regge trajectory was taken as $\alpha_{\omega, \rho}(t) = 0.45 + 0.9t$, with $s_0 = 1$ GeV². The parameters $\gamma_1 = 115.4(3.7)\sqrt{\mu b}$, $\gamma_1^{\text{cut}} = 55.2(5.7)\sqrt{\mu b}$, $\gamma_3^{\text{cut}} = 13.5(0.8)\sqrt{\mu b}/\text{GeV}$, $a = 1.20$ GeV⁻²,⁴ and $\Gamma_{\gamma\gamma} = 8.44$ eV represent the best fit values to the available experimental data [25]; $G_E(t)$ is the electric dipole proton form factor.⁵

The results of the elementary photoproduction parametrization with and without the Coulomb contribution are shown in Fig. 2. The data were taken from [25,26] where the solid histograms represent our Monte Carlo generated input.

⁴This value is slightly higher than the value of [25] to better fit the data at larger angles.

⁵The magnetic part of the Coulomb amplitude goes with t and do not contribute for low scattering angles.

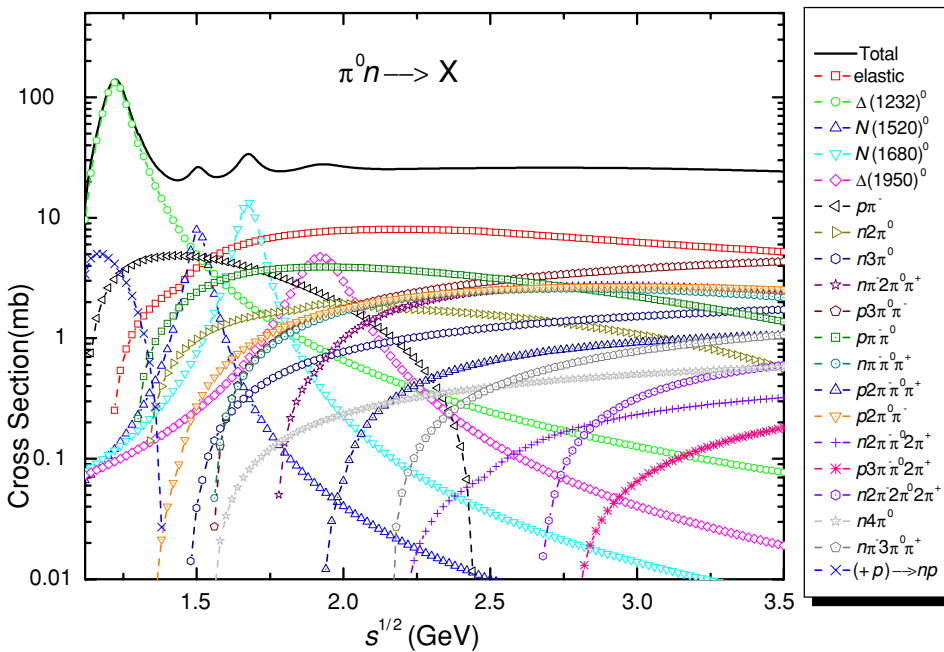


FIG. 3. (Color online) Total $\pi^0 n$ cross section and respective branching ratios as a function of the total energy in the πN center-of-mass frame.

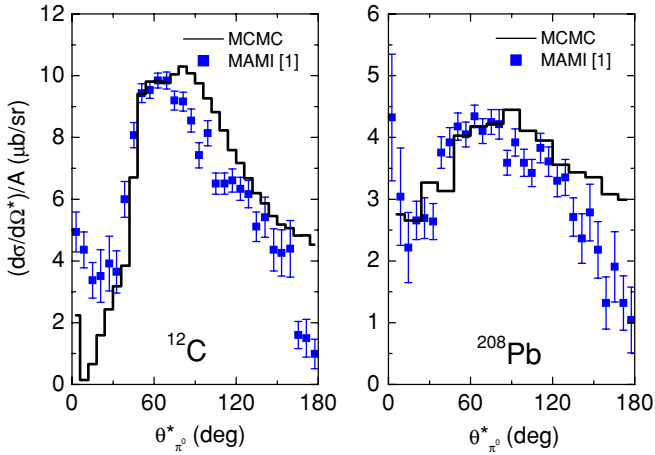


FIG. 4. (Color online) Incoherent π^0 photoproduction from ^{12}C and ^{208}Pb for $E_\gamma = 0.33$ GeV in the γ + nucleus center-of-mass frame. The data points were taken from Ref. [1].

The π nucleus FSI is realistically taken into account via a dynamical analysis of multiple πN scattering processes. This time-dependent analysis propitiates a unique approach to deal with the in-medium modifications in meson production, as it naturally updates the local density fluctuations in time. The Pauli-blocking mechanism prevents spurious scatterings whenever the nucleon final state is already occupied. In summary, the following πN scatterings are included: (i) elastic scattering, (ii) resonance production and decay, (iii) charge exchange processes, (iv) π reabsorption by a nucleon pair, and (iv) multiple π^0 and $\pi^{+,-}$ production processes. The cross sections for the entrance channels $\pi^+ p$ and $\pi^- p$ were extracted from the Particle Data Group (PDG) database and fitted from the thresholds to 6 GeV assuming a combination of a Lorentz shape, whenever a resonance contribution exists, with a smooth

function of the total energy of the πN system in the center-of-mass frame of the s -channel. For the remaining entrance channels $\pi^+ n, \pi^- n, \pi^0 p, \pi^0 n$, we have assumed conservation of isotopic spin, strangeness, and parity and that the strong interaction is invariant under charge conjugation and time reversal. Within this prescription, we accurately estimate the total πN cross section for all these channels. The usefulness of this new methodology is shown in Fig. 3, where we have plotted our results for the particular neutral channel $\pi^0 n$. For low energies ($\sqrt{s} \approx 1.2$ GeV), the Δ excitation largely dominates the branching ratios, and other mechanisms such as charged exchange scatterings are always contributing within 3%. This reinforces our previous assumptions that direct charged pion photoproduction do not contribute significantly to neutral pions. For higher energies ($\sqrt{s} \gtrsim 2$ GeV), however, multiple particle production is more relevant.

The incoherent differential cross sections for single π^0 photoproduction from nuclei can be written as follows:

$$\frac{d\sigma_A}{d\Omega}(E_\gamma, \theta) = A\xi(E_\gamma, \theta)f(Q) \times \frac{d\sigma_N}{d\Omega}(E_\gamma, \theta)[1 + \lambda(E_\gamma, \theta)], \quad (13)$$

where A is the nucleus mass, θ is the polar angle, ξ is the π^0 nuclear absorption, f is the Pauli-blocking suppression factor for small momentum transfer Q , $d\sigma_N/d\Omega$ is the photoproduction from the nucleon⁶ and λ is a factor accounting for the π^0 secondary production and rescattering.

⁶This elementary operator is given in terms of the two particular choices of the photoproduction mechanisms given by Eqs. (1) and (8).

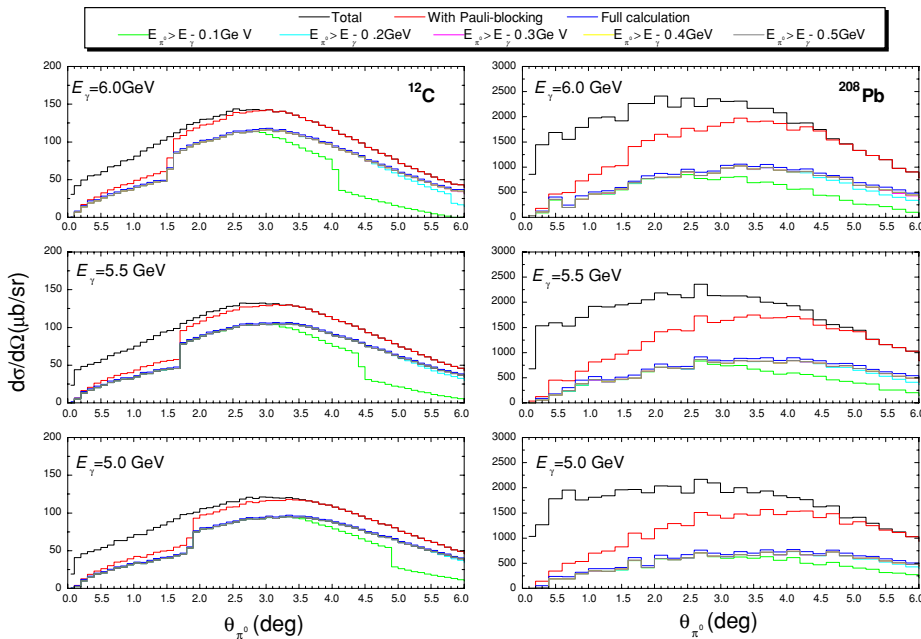


FIG. 5. (Color online) Incoherent π^0 photoproduction from ^{12}C and ^{208}Pb at forward angles and high energies: $5.0 \leq E_\gamma \leq 6.0$ GeV. Total cross section (black), with Pauli-blocking (red) and with Pauli-blocking plus FSI (blue). The kinematical cuts are as follows: $E_{\pi^0} > E_\gamma - 0.1$ GeV (green), $E_{\pi^0} > E_\gamma - 0.2$ GeV (cyan), $E_{\pi^0} > E_\gamma - 0.3$ GeV (magenta), $E_{\pi^0} > E_\gamma - 0.4$ GeV (yellow), and $E_{\pi^0} > E_\gamma - 0.5$ GeV (gray).

The calculations of the incoherent π^0 differential cross sections for ^{12}C and ^{208}Pb at $E_\gamma = 0.33$ GeV are shown in Fig. 4, together with recent results from MAMI [1]. The agreement between our calculations and the experiment is remarkable, even for the steep increase of the cross section for ^{12}C in the range $30^\circ \lesssim \theta \lesssim 60^\circ$. This feature is most probably due to the spin-orbit coupling of the $p_{1/2}$ and $p_{3/2}$ shells during the photoproduction, and its reproduction reflects the accurate momentum distribution used in our calculations. For ^{208}Pb , however, we have obtained a much broader distribution, typical of a Fermi gas. The cross section peak is reduced by a factor of ~ 2 for ^{12}C and ~ 4 for ^{208}Pb , indicating a much stronger FSI effect for ^{208}Pb , as expected from phenomenological considerations. Some discrepancies appear at forward and backward angles, where the former is most likely attributed to the additional incoherent pions generated from coherent production thru FSI.

In Fig. 5 we show our results for the incoherent π^0 production at small angles in the energy range $5.0 \leq E_\gamma \leq 6.0$ GeV. Different kinematical cuts to the total pion energy

E_π were applied, because for both Coulomb and nuclear coherent photoproductions we have $E_\pi \approx E_\gamma$ (no recoil approximation). The average number of interactions of *all* the produced pions before exiting the nucleus, for a typical incident energy of 6 GeV, is ~ 0.4 and ~ 5.5 for ^{12}C and ^{208}Pb , respectively. In fact, this new approach provides a feasible and sophisticated dynamical calculation because many steps of interactions are effectively included.

In summary, a full calculation of the incoherent π^0 photoproduction from nuclei, based on a time-dependent intranuclear cascade Monte Carlo approach, has been introduced. Differently from Monte Carlo event generators, which neglect the evolution of the nuclear state, this calculation takes into account the whole nucleus configuration, making it a powerful tool to elucidate in-medium effects in meson photoproduction in a wide energy and mass range.

The authors thank the Brazilian agencies FAPESP and CNPq and the Latin-American Physics Center (CLAF) for partial support to this work.

-
- [1] B. Krusche *et al.*, Eur. Phys. J. A **22**, 277 (2004).
 [2] H. Primakoff, Phys. Rev. **81**, 899 (1951).
 [3] A. Browman, J. De Wire, B. Gittelman, K. M. Hanson, D. Larson, E. Loh, and R. Lewis, Phys. Rev. Lett. **33**, 1400 (1974).
 [4] A. Gasparian *et al.*, *A Precision Measurement of the Neutral Pion Lifetime via the Primakoff Effect*, The PrimEx experiment at Jlab, Proposal E-02-103 (2002).
 [5] C. A. Engelbrecht, Phys. Rev. **133**, B988 (1964).
 [6] M. G. Gonçalves, S. de Pina, D. A. Lima, W. Milomen, E. L. Medeiros, and S. B. Duarte, Phys. Lett. **B406**, 1 (1997).
 [7] M. G. Gonçalves, E. L. Medeiros, and S. B. Duarte, Phys. Rev. C **55**, 2625 (1997).
 [8] S. de Pina, E. C. Oliveira, E. L. Medeiros, S. B. Duarte, and M. Gonçalves, Phys. Lett. **B434**, 1 (1998).
 [9] S. B. Duarte (private communication).
 [10] T. E. Rodrigues, J. D. T. Arruda-Neto, A. Deppman, V. P. Likhachev, J. Mesa, C. Garcia, K. Shtejer, G. Silva, S. B. Duarte, and O. A. P. Tavares, Phys. Rev. C **69**, 064611 (2004).
 [11] A. Boudard, J. Cugnon, S. Leray, and C. Volant, Phys. Rev. C **66**, 044615 (2002).
 [12] M. Effenberger, E. L. Bratkovskaya, and U. Mosel, Phys. Rev. C **60**, 044614 (1999).
 [13] J. Lehr, M. Effenberger, and U. Mosel, Nucl. Phys. **A671**, 503 (2000).
 [14] D. Drechsel, O. Hanstein, S. S. Kamalov, and L. Tiator, Nucl. Phys. **A645**, 145 (1999).
 [15] F. Härter, Ph.D. thesis, Mainz University (1996).
 [16] G. Fischer, H. Fischer, G. von Holtey, H. Kampgen, G. Knop, P. Schulz, and H. Wessels, Z. Phys. **245**, 225 (1971).
 [17] H. Genzel *et al.*, Z. Phys. **268**, 43 (1974).
 [18] R. Beck *et al.*, Phys. Rev. Lett. **78**, 606 (1997).
 [19] J. Ahrens *et al.*, Eur. Phys. J. A **21**, 323 (2004).
 [20] W. Braunschweig, H. Genzel, and R. Wedemeyer, Z. Phys. **245**, 253 (1971).
 [21] J. S. Ball, Phys. Rev. **124**, 2014 (1961).
 [22] G. F. Chew, M. L. Goldberger, F. E. Low, and Y. Nambu, Phys. Rev. **106**, 1345 (1957).
 [23] A. Gasparian and S. Gevorkyan (private communication).
 [24] J. S. Ball, W. R. Frazer, and M. Jacob, Phys. Rev. Lett. **20**, 518 (1968).
 [25] M. Braunschweig, W. Braunschweig, D. Husmann, K. Lübelmeyer, and D. Schmitz, Nucl. Phys. **B20**, 191 (1970).
 [26] R. L. Anderson, D. B. Gustavson, J. R. Johnson, I. D. Overman, D. M. Ritson, B. H. Wiik, and D. Worcester, Phys. Rev. D **4**, 1937 (1971).